Structure and order of a homologous series of bent-core molecules: A ^{13}C NMR study

Ronald Y. Dong,[1,2] J. Xu,[1] G. Benyei,[3] and K. Fodor-Csorba[4]

[1]*Department of Physics and Astronomy, University of Manitoba, Winnipeg, MB, Canada R3T 2N2*

[2]*Department of Physics and Astronomy, Brandon University, Brandon, MB, Canada R7A 6A9*

[3]*Department of Organic Chemistry, University Eötvös Loránd, P.O. Box 49, H-1117 Budapest, Hungary*

[4]*Research Institute of Solid State Physics and Optics, Hungarian Academy of Sciences, P. O. Box 49, H-1525 Budapest, Hungary*

A carbon-13 NMR study in a series of bent-core (banana-shaped) molecules is reported. In 1,3-phenylene bis[4′-alkenyloxy biphenyl]-4-carboxylate derivatives the position of the chlorine substitutent(s) connected to the central phenly ring and/or the terminal chain length of the compounds were varied. By analyzing the observed chemical shift anisotropies, the order parameters S and bending angles in their nematic phase are compared. The biphenyl moiety on each arm of the molecular core is found to form a nonzero twist angle.
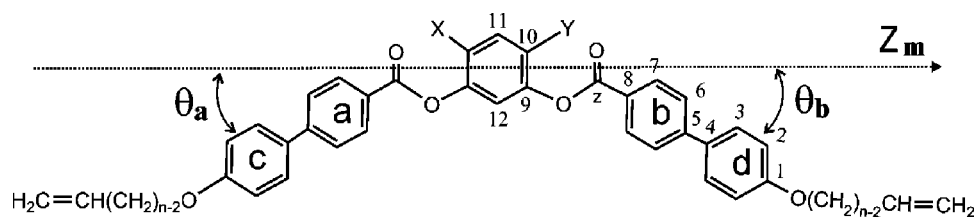
PACS number(s): 61.30.−v

I. INTRODUCTION

Tilted smectic phases of liquid crystals that show chiral properties due to breaking of mirror symmetry have attracted much attention in recent years. The constituent molecules can either possess molecular chirality due to the presence of asymmetric carbon(s) [1–3] or are achiral as shown by bent-core or banana-shaped mesogens [4]. The former class can exhibit ferroelectric, antiferroelectric, and ferri smectic phases in which a spontaneous electric polarization $\vec{P}$ appears in each layer. Bent-core molecules do not have cylindrical symmetry, thus requiring two unit vectors $\hat{n}$ and $\hat{m}$ for their description. The vector $\hat{m}$ is normal to the average molecular plane, while $\hat{n}$ is along the long axis of the molecule (the director). Each layer is polar because of the efficient packing of the molecules. The electric polarization is along the unit vector $\hat{b}$, which is normal to both $\hat{n}$ and $\hat{m}$ vectors when the achiral molecule has a C_{2v} symmetry. When molecules tilt away from the layer normal $\hat{k}$ at a tilt angle θ, which is measured by $\hat{n} \times \hat{k} = \sin \theta = |\vec{\xi}|$. Now the vectors $\vec{P}$ and $\vec{\xi}$ form an angle ψ. Thus all tilted banana (B) phases can be specified by the angles θ and ψ [5]. Indeed, the tilt direction of molecular planes and the polar order axis are the two independent symmetry breaking factors; the chirality can be defined by $\chi = 2[(\hat{k} \times \hat{n}) \cdot \hat{b}](\hat{k} \cdot \hat{n})$ [6]. While there is an enormous scientific interest in these achiral materials, there seems to be a huge potential for high-tech applications as well, e.g., ferroelectricity and antiferroelectricity for electro-optical applications. Electro-optical switching has indeed been observed in B_2 and B_5 phases [7]. Structure and dynamics of banana mesogens and in particular the so-called B phases are the subject of intense research. Several classes of banana molecules have been synthesized in the last five years [8–10]. Many of them were based on resorcinol as the central unit. Introduction of substituents at different positions either on the central or on the outer aromatic rings leads to a conformational change of the whole molecule and naturally alters the bending angle Ψ of the mesogenic core units. It has often been stated that such materials, consisting of achiral molecules, may form chiral smectic layers, but nematic phase is seen in increasing number of compounds.
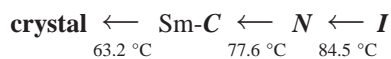
Few papers concerning ^{13}C NMR investigations on banana-shaped molecules have been published in the last few years [11–14] showing the possibility to access geometrical information, such as the bending angle. However, these studies have revealed that the analyses of ^{13}C NMR spectra need the knowledge of the orientation and chemical shift anisotropy (CSA) tensor of each carbon in the molecule. Incorrect CAS tensorial quantities could introduce non-negligible errors in either the local order parameter S_{zz} or the molecular geometry. ^{1}H and ^{19}F NMR have been introduced [15] to support ^{13}C NMR studies. More recently, ^{2}H and ^{13}C NMR spectroscopies are combined to give precise structural information of the banana-shaped mesogen 4-Chloro-1, 3-phenylene bis[4′-(10-undecenyloxy)benzoyloxy]-4-benzoate (ClPbis11BB) in its nematic phase [16]. The synthesis of this compound was first reported in Ref. [10]. In the same study, quantum chemical calculations have also been used to shed light on the molecular conformation of the five-ring molecular core. In this study, we report on a ^{13}C study of the banana-shaped mesogens 4-Chloro-1,3-phenylene bis [4′-(10-undecen-1-yloxy)-1,1′-biphenyl]-4-carboxylate [11 ClPBBC] and its related analogs 4,6-dicholoro-1,3-phenylene bis[4′-(9-decen-l-yloxy)-l,4′-biphenyl]-4-carboxylate [10DClPBBC] and 4,6-dichloro-1,3-phenylene bis[1′-(10-undecen-1-yloxy)-1,1′-biphenyl]-4-carboxylate [11DClPBBC]. These latter compounds differ from the former ClPbis11BB by the lack of one ester–COO linking group in each wings of the molecules. By varying the substituents in the central phenyl ring, it is our aims to probe the molecular structure and order parameters of these banana-shaped molecules in the nematic phase.

II. EXPERIMENT

Figure 1 shows the molecular structure of studied banana-shaped molecules given below. Their phase transition temperatures as observed by polarization microscopy as well as their clearing temperatures (t_c) as determined by NMR are the following:
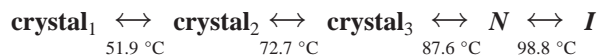
FIG. 1. Molecular structure of nClPBBC or nDClPPBC and its long molecular axis z_M. The bending angle $\Psi = 180° - (\theta_a + \theta_b)$, where θ_i is the angle between the para axes of a biphenyl fragment and the z_M axis.

4-Chloro-1,3-phenylene bis[4′-(10-undecen-1-yloxy)-1,1′-biphenyl] carboxylate [11ClPBBC]

$$\textbf{crystal} \underset{63.2\,°C}{\longleftarrow} \textbf{Sm-}\textit{C} \underset{77.6\,°C}{\longleftarrow} \textit{N} \underset{84.5\,°C}{\longleftarrow} \textit{I}$$

$$X = Cl, \ Y = H, n = 11; t_c = 86\,°C$$

4,6-Dichloro-1,3-phenylene bis[4′-(9-decen-1-yloxy)-1,1′-biphenyl] carboxylate [10DClPBBC]

$$\textbf{crystal}_1 \underset{51.9\,°C}{\longleftrightarrow} \textbf{crystal}_2 \underset{72.7\,°C}{\longleftrightarrow} \textbf{crystal}_3 \underset{87.6\,°C}{\longleftrightarrow} \textit{N} \underset{98.8\,°C}{\longleftrightarrow} \textit{I}$$

$$X = Cl, Y = Cl, n = 10; t_c = 100.5\,°C$$

4,6-Dichloro-1,3-phenylene bis[4′-(10-undecen-1-yloxy)-1,1′-biphenyl] carboxylate [11DClPBBC]

$$\textbf{crystal}_1 \underset{71.2°C}{\longleftrightarrow} \textbf{crystal}_2 \underset{78.6°C}{\longleftrightarrow} \textit{N} \underset{10.27°C}{\longleftrightarrow} \textit{I}$$

$$X = Cl, Y = Cl, n = 9; T_c = 104\,°C$$

The synthesis of the studied bent-core compounds will be described elsewhere [17]. The ^{13}C NMR experiments were performed on a Bruker Avance 400 spectrometer operating at 100.6 MHz. The one-dimensional (1D) and 2D ^{13}C NMR spectra of the banana samples in CDCl$_3$ were performed in the high-resolution (HR) mode using a broadband invase (BBI) probe. The 1D ^{13}C spectrum was obtained by using a single carbon pulse and the free induction decay (FID) collected with the Waltz-16 proton decoupling sequence. The ^{13}C peak assignments were aided by the well-known distortionless enhancement by polarization transfer (DEPT) and 2D ^{13}C-^1H correlation (XHCORR) experiments [18]. The 1D ^{13}C NMR experiments of the static neat sample were done with a two-channel HX solid probe. The isotropic phase spectrum was collected as in the HR mode except the Waltz-16 decoupling power was higher. The ^{13}C spectra in the nematic phase were collected using standard CP (cross polarization) for 2 ms after the 90° proton irradiation. Proton decoupling during the ^{13}C signal acquisition was done by the SPINAL-64 pulse sequence [19] with a minimal decoupling field of ca. 10 kHz. To avoid sample heating, the recycle delay between each FID acquisition was 6 s. Each spectrum was obtained after signal averaging 512 or 256 scans. The temperature calibration was made for a given air flow using the known phase transition temperatures of a liquid crystal. The ^{13}C peak assignments in the aligned sample were based on experiments using the pulse sequence with phase inversion (PI) and CP (i.e., CPPI) [20]

and previous ^{13}C peak assignments in similar compounds [16,21,22]. In the CPPI spectrum, one should see negative CH$_2$, null CH, and positive nonprotonated C signals. The ^1H 90° pulse width was 3.4 μs and the temperature gradient across the sample was estimated to be within 0.3°C.

III. RESULTS AND DISCUSSION

Figure 2 shows the HR ^{13}C NMR spectra of 11ClPBBC/CDCl$_3$ solution together with the ^{13}C peak assignments. The bottom trace is a DEPT spectrum in which CH$_2$ signals are negative, CH signals positive, and null signals for all nonprotonated carbons. Figure 3 shows a 2D HXCORR spectrum of 11ClPBBC/CDCl$_3$ and its 1D ^1H and ^{13}C spectra on the sides. Isotropic chemical shifts of protons were assigned first in its HR proton spectrum, and the peak assignments in the HXCORR spectrum are according to the ^1H and ^{13}C isotropic chemical shifts. The corresponding HR spectra of 10DClPBBC and 11DClPBBC are similar. Typical ^{13}C spectra obtained in static samples of 10DClPBBC and 11ClPBBC at several temperatures are shown in Figs. 4 and 5, respectively. The ^{13}C spectra of 11DClPBBC are almost identical to those shown in Fig. 4. The aligned sample in the magnetic field was obtained by cooling from the isotropic (I) phase to the nematic (N) phase. During the phase transition
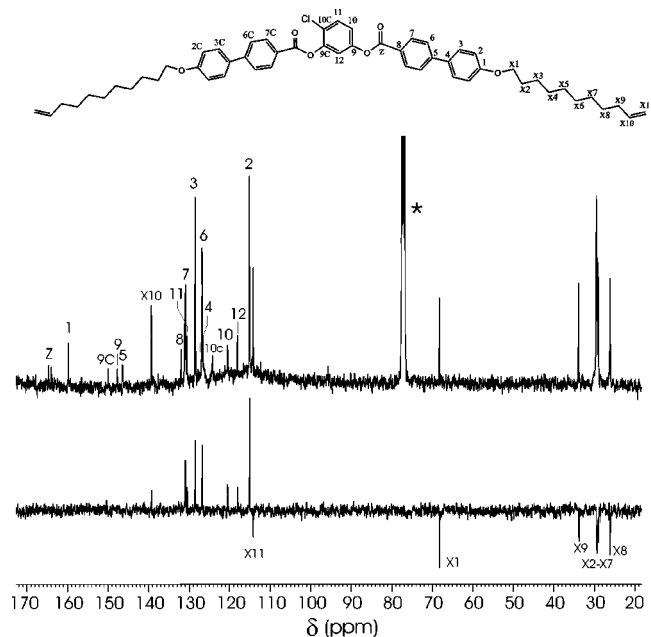

FIG. 2. High-resolution ^{13}C spectrum of 11ClPBBC/CDCl$_3$ solution at ambient temperature and its corresponding DEPT spectrum (bottom trace). The asterisk denotes an impurity peak.
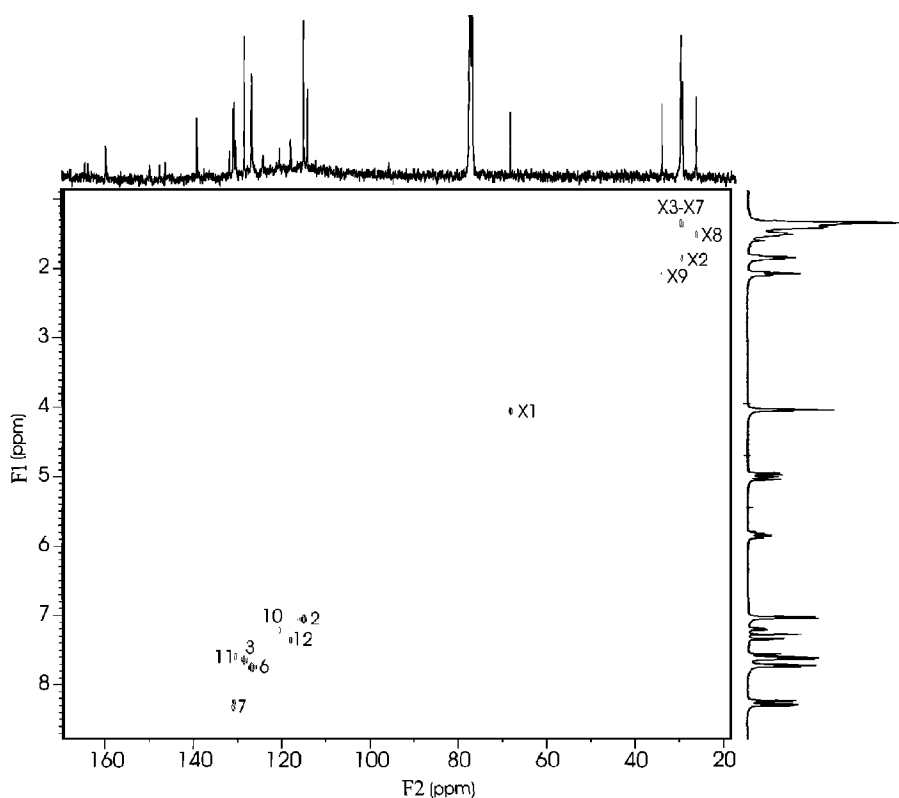
FIG. 3. Two-dimensional HXCORR spectrum of 11ClPBBC/CDCl$_3$ at ambient temperature.
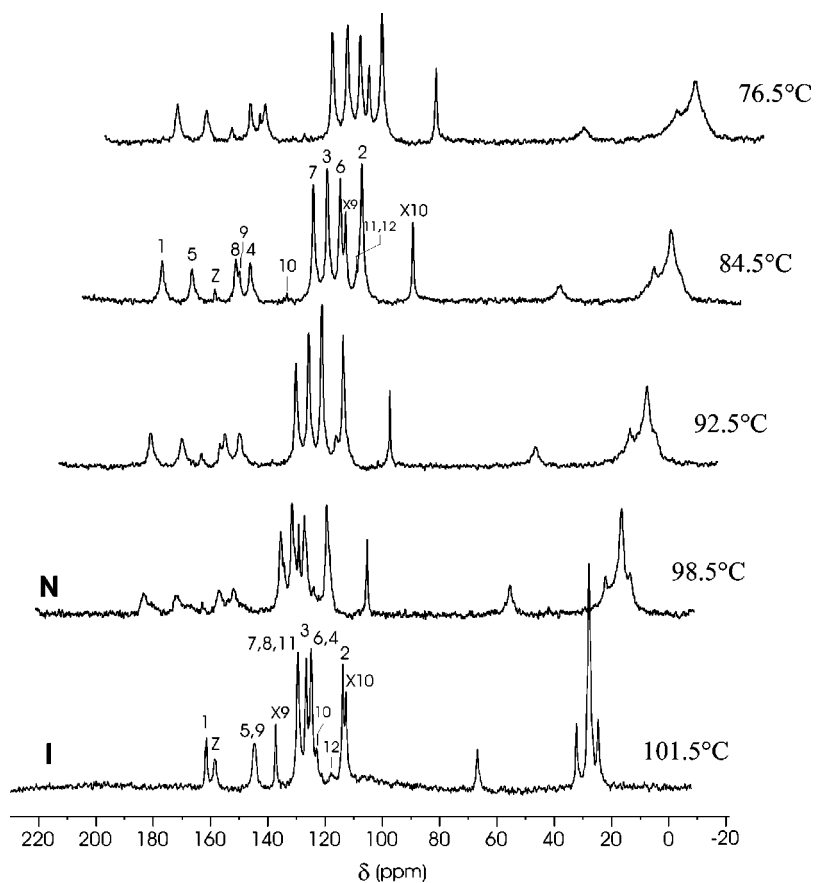

FIG. 4. Typical ^{13}C spectra observed in the aligned sample of 10DClPBBC at several temperatures by cooling form the isotropic phase.
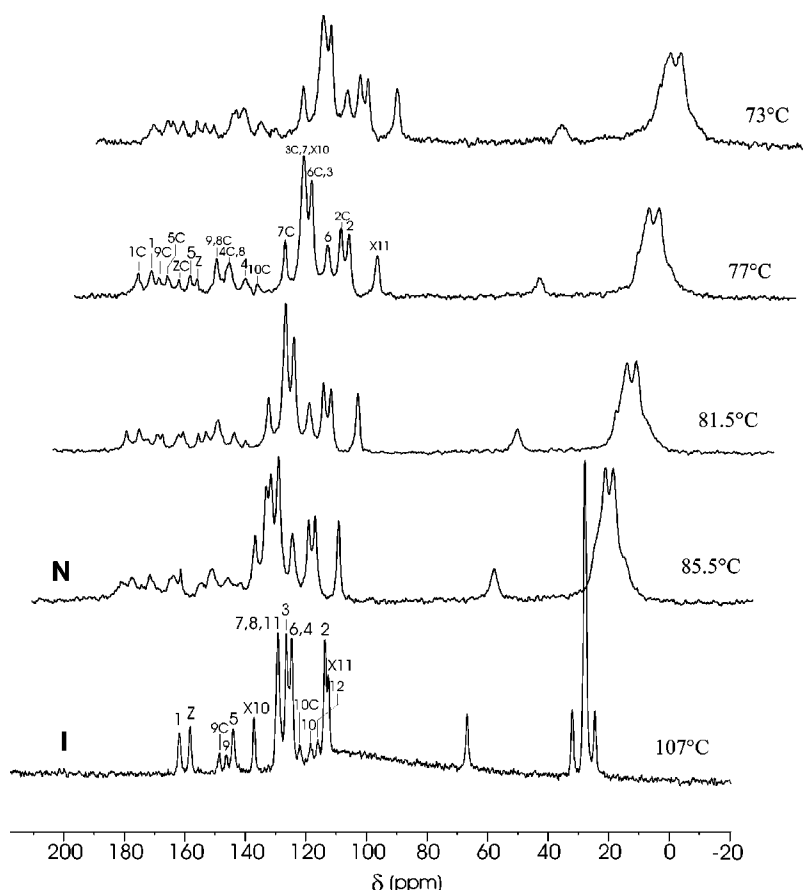
FIG. 5. Typical ^{13}C spectra observed in the aligned sample of 11ClPBBC at several temperatures by cooling from the isotropic phase.

from I to N, ^{13}C chemical shifts $\sigma^{(j)}$ of the aromatic carbons shift markedly downfield but those of the aliphatic carbons shift slightly upfield. It is clear that the aliphatic carbon peaks are closely overlapped except X9 (X10) and X10 (X11), and the present ^{13}C study, therefore, focuses on the aromatic carbons to extract both the orientational ordering of the banana core and its "average" molecular structure in the nematic phase. Figures 6–8 show the temperature dependences of $\delta^{(j)}$ for the aromatic carbons, X9 (X10) and X10 (X11) carbons for our three samples. It is noted that the δ temperature dependences of X9, X10, and X11 carbons are rather weak, and the carbon peak assignments for the central phenyl ring are tentative.

The chemical shift δ in a liquid crystalline phase is related to the isotropic chemical shift δ_{iso}, the components of the chemical shift tensor δ_{ij}, and order parameter S_{ij} according to [23]

$$\delta = \delta_{iso} + \frac{2}{3}S_{zz}\{\delta_{zz} - (\delta_{xx} + \delta_{yy})/2\} + \frac{1}{3}(\delta_{xx} - \delta_{yy})(S_{xx} - S_{yy})$$

$$+ \frac{2}{3}(S_{yz}\delta_{yz} + S_{xz}\delta_{xz} + S_{xy}\delta_{xy}). \tag{1}$$

Because of rapid rotations of the molecule about its long molecular axis (e.g., z_M axis in Fig. 1), S_{xy}, S_{yz}, and S_{xz} vanish, and $S_{xx}-S_{yy}$ is usually small in uniaxial mesophases. With these restrictions,

$$\delta = \delta_{iso} + \frac{2}{3}S(\delta_{\parallel} - \delta_{\perp}), \tag{2}$$

where $\delta_{\parallel}$ is the chemical shift component along the direction of the z_M axis, $\delta_{\perp} = (\delta_{xx} + \delta_{yy})/2$ is the average chemical shift component along a short molecular axis, and S is the order parameter associated with the (assumed) long molecular axis. In the simple case of a rapid rotation about the long axis, $\delta_{\parallel}$ and $\delta_{\perp}$ are given by

$$\delta_{\parallel} = (\cos^2\alpha \cos^2\beta)\delta_{11} + (\sin^2\alpha \sin^2\beta)\delta_{22} + (\cos^2\beta)\delta_{33},$$

$$\delta_{\perp} = \frac{1}{2}(1 - \cos^2\alpha \sin^2\beta)\delta_{11} + \frac{1}{2}(1 - \sin^2\alpha \sin^2\beta)\delta_{22}$$

$$+ \frac{1}{2}\sin^2\beta\delta_{33}, \tag{3}$$

where α and β are the polar angles for δ_{ij} in the molecular (x_M, y_M, z_M) frame. To derive S from Eqs. (2) and (3), the CSA tensor components δ_{ij} must be known for various carbon sites. The principal axis $(1,2,3)$ frame of the CSA tensor must also be known and is chosen in this study by assuming that the 3-axis is along the C-H bond or C-C bond, and the l-axis is normal to the central phenyl ring plane. The assumption is made necessary by the fact that the CSA tensors and their orientations are unavailable for carbons on these banana-shaped molecules. Because of the lack of suitable CSA tensors for the carbons in the central phenyl ring in
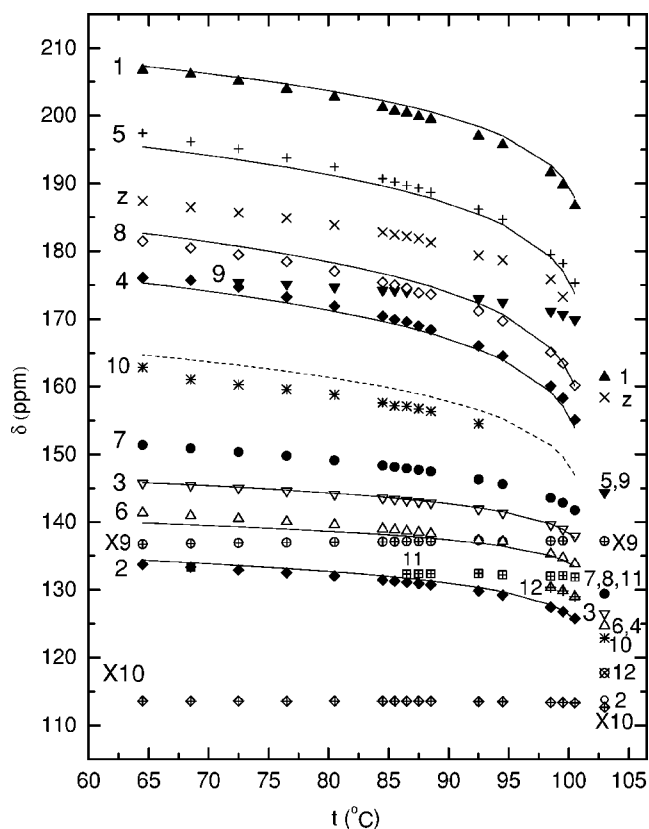
FIG. 6. Plots of chemical shifts of the aromatic carbons and aliphatic carbons X9 and X10 in the isotropic and nematic phases of 10DClPBBC. The carbon labels are indicated in Fig. 2 except that the chain is shorter and C_{10} has a Cl atom instead.

FIG. 7. Plots of chemical shifts of the aromatic carbons and aliphatic carbons X10 and X11 in the isotropic and nematic phases of 11DClPBBC.

the literature and the uncertainty in their assignments in the ^{13}C spectra, we have concentrated on fitting the chemical shifts data of C_1–C_8 (except C_7 whose CSA tensor is uncertain) from the two biphenyls (a,c or b,d in Fig. 1) in each banana-shaped molecule. It is noted that the *para* axes of biphenyl rings are collinear, and these rings are known to perform rapid ring flips about their para axes. The ^{13}C chemical shift data can be used to determine the local order parameter S, plus the angles θ_a and θ_b each biphenyl para axes formed with respect to the z_M axis. To calculate the chemical shifts $\delta^{(j)}$ of carbons on these rings, there is an additional coordinate transformation from the *para* axes (x_p, y_p, z_p) to the molecular z_M axis resulting in the following expression:

$$\delta^{(j)} = \delta_{iso}^{(j)} + \frac{2}{3} S P_2(\cos \theta_i) \left[\left(-\frac{1}{2} + \frac{3}{2} \cos^2 \alpha^{(j)} \sin^2 \beta^{(j)} \right) \delta_{11}^{(j)} \right.$$
$$\left. + \left(-\frac{1}{2} + \frac{3}{2} \sin^2 \alpha^{(j)} \sin^2 \beta^{(j)} \right) \delta_{22}^{(j)} + P_2(\cos \beta^{(j)}) \delta_{33}^{(j)} \right].$$
$$(4)$$

Here $\alpha^{(j)}$ and $\beta^{(j)}$ are the polar angles for the $\delta_{ij}^{(j)}$ of the jth carbon in the (x_p, y_p, z_p) frame. The x_p-z_p plane is defined by the plane of the central phenyl ring. As seen in Fig. 5, the carbon signals from the biphenyl fragments (1–8) show
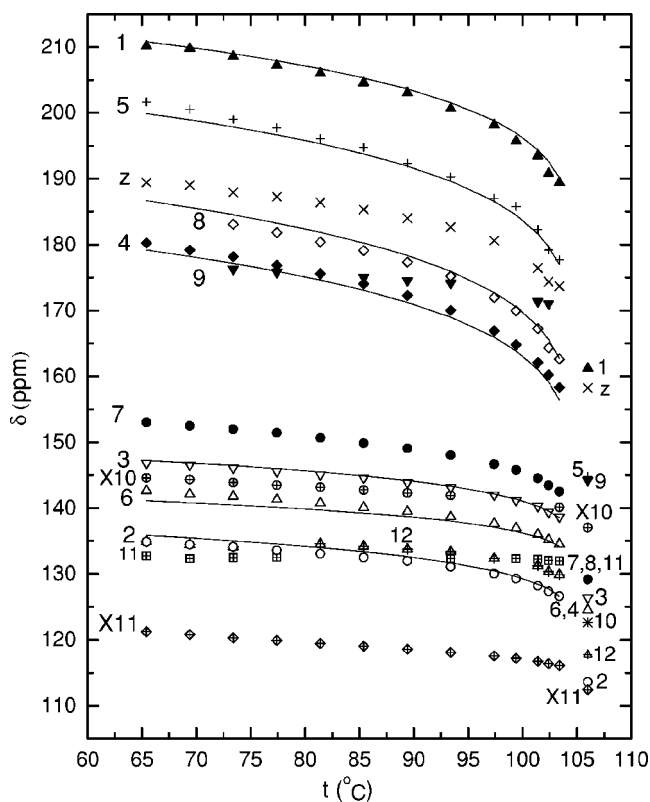
clearly doubling in 9ClPBBC—i.e., 1 and 1c, etc., at 77 °C for the monosubstituted banana. Thus the ^{13}C signals of the biphenly moiety in this banana-shaped mesogen are different for the two *lateral* wings indicating that their *para* axes make quite different θ_i angles. This is consistent with the deuterium data of ClPbis11BB, which is also a monosubstituted banana [16]. In the 9ClPBBC compound $\theta_a = \theta_{Cl}$ and $\theta_b = \theta_H$; for the other two disubstituted compounds, $\theta_a = \theta_b = \theta_{Cl}$. When all rings in the wings are coplanar with the central ring, then $\alpha = 90°$ in the above equation. Now the phenyl rings in the biphenyl are known to twist with respect to each other with a twist angle ϕ. We have, therefore, allowed rings a and b to rotate away from the planar conformation. As a result, for carbons on them the angle $\alpha = 90°$-ϕ. In an attempt to use Eq. (4) to estimate order and geometry of the banana core from various carbon sites in the *lateral* rings, we note that the general features of CSA tensors have been given for aromatic carbons of model compounds (including a model LC compound) in the literature [21,24,25]. These are tabulated in Table I together with calculated δ_{iso} values for direct comparison with experimental values in the isotropic phase. For the protonated carbon, the β angle between the C-H bonds and the *para* axis of each ring has the nominal value of 60°. For the *para* carbons, $\beta = 0$. As seen in Eq. (4), the change in the chemical shift $\Delta \delta^{(j)}$ can only give the product S and $P_2(\cos \theta_i)$ and our data from the biphenyl fragments cannot untangle the order parameter S and the angle θ_i unambiguously. We have therefore chosen to set θ_{Cl} equal to an average value of 12° as determined from the deuteron
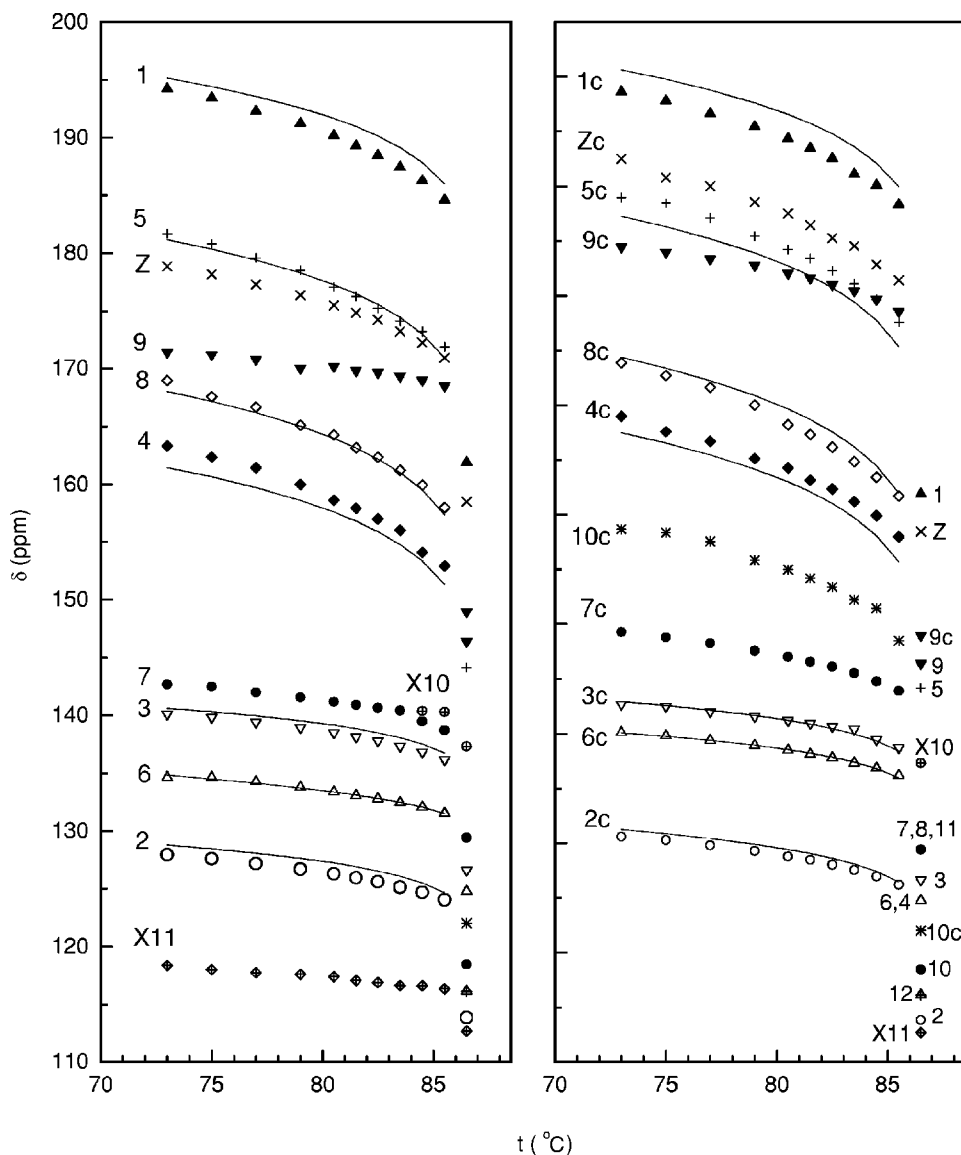
FIG. 8. Plots of chemical shifts of the aromatic carbons and aliphatic carbons X10 and X11 in the isotropic and nematic phases of 11ClPBBC. The carbon labels are indicated in Fig. 2.

results in ClPbisBB [16]. Now by fitting the observed chemical shifts at each temperature, one can calculate S for each carbon site and the unknown angle θ_H in the case of 11ClPBBC, as well as the twist angles ϕ_a and ϕ_b. We found that θ_H, ϕ_a, and ϕ_b are weakly temperature sensitive. We have carried out a global target analysis of all the $\Delta\delta'$s for the C_1–C_8 and/or C_{1c} and C_{8c} given in Figs. 6–8 to obtain

TABLE I. CSA tensors for various carbon sites (site labels are for both *lateral* wings).

Sites	1[a]	2[b]	3[a]	4[b]	5[a]	6[a]	8[c]
δ_{11}	67.8	8.7	21.8	14.6	20	21.3	8.7
δ_{22}	169.3	135.5	145.5	147.4	173	150.2	155.7
δ_{33}	244	192.6	217.9	219.3	236	200.8	227.7
δ_{iso}	160.4	112.2	128.4	127.1	143	124.1	130.7

[a]Reference [21].
[b]Reference [24].
[c]Reference [25].

S, ϕ_a, and ϕ_b, as well as θ_H, for the case of 11ClPBBC by minimizing the sum square errors using the routine AMOEBA [26]. To do this, we have adopted the temperature dependence of S using the Haller equation [27]

$$S(T) = S_0(1 - T/T^*)^f,$$

where S_0 and f are empirical constants and T^* is the temperature slightly above T_c at which S becomes zero. We have set $T^* = T_c + 1$ K, and the weak temperature behavior in angles Ω_i is modeled by a general linear equation $\Omega_i = \Omega_i' + \eta_i(T - T_c)$. In our initial global analyses, S_0, f, Ω_i', and η_i are the variables to give the best fits of the chemical shifts at a number of temperatures (15 for 10DClPBBC, 13 for 11DClPBBC, and 10 for 11ClPBBC). For final analyses, we have chosen to use an "average" molecular structure for each banana core. In the case of 11ClPBBC, this was done in a two-step process: once the average θ_H was found, a second global analysis with variable ϕ_a and ϕ_b was done in order to find their average values for final global analysis. For the other two samples, there is no θ_H. It is noted that the em-
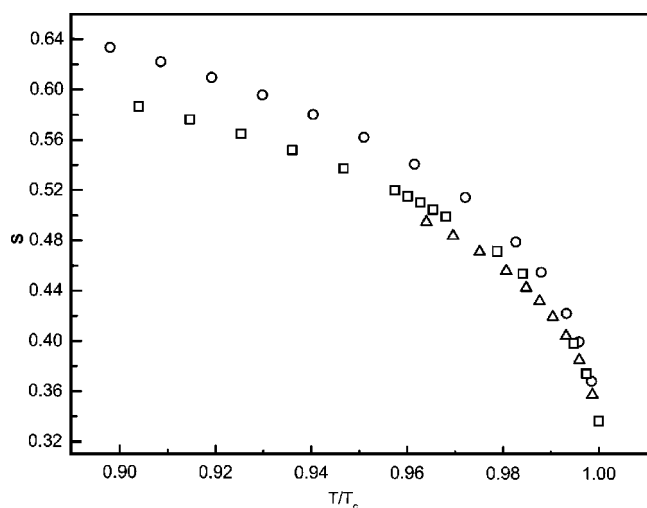
FIG. 9. Plots of the order parameter S as a function of reduced temperature for 10DClPBBC (squares), 11DClPBBC (circles), and 11ClPBBC (triangles).

ployment of average molecular structure did not adversely affect the fits. Furthermore, the derived S as a function of temperature is more or less unchanged. The calculated δ's are shown as solid curves in Figs. 6–8. As seen in these figures the experimental chemical shifts in the nematic phase for the studied sites are reproduced satisfactorily. Figure 9 summarizes the local order parameter S of the molecular core for the studied banana-shaped molecules as a function of the reduced temperature. For 10DClPBBC and 11DClPBBC, the S can be identified as the nematic order parameter for the core. Since the two lateral arms are not symmetric with respect to the central phenyl ring in 11ClPBBC, our calculated S reflects more for the ordering of the central ring. Now $S_0 = 0.79$ and $f = 0.145$ in 11ClPBBC, while the corresponding values for 10DClPBBC and 11DClPBBC are, respectively, $0.84, 0.153$ and $0.93, 0.168$. It is interesting to note that the S values T_c are almost identical for the three related banana-shaped mesogens, even though the empirical constants in the Haller equation are different. The average θ_H angle and the average twist angels ϕ_a and ϕ_b for 11ClPBBC are 21.2°, 13.5°, and 24.2°, respectively. The average twist angles ($\phi_a = \phi_b$) for 10DClPBBC and 11DClPBBC are almost identical, 19.9°, and 19.5°, respectively. The bending angle Ψ subtended by the two side wings in the monosubstituted banana-

shaped molecule 11ClPBBC (146.8°) is smaller than the disubstituted molecules (156°) by about 9°. They are, however, significantly larger than the value of 127.6° reported for another banana-shaped molecule [28]. In summary the present ^{13}C results show how the average structure and ordering of the bent-core in banana-shaped mesogens can be obtained.

IV. CONCLUSION

The present study shows that carbon-13 NMR can provide useful information on the molecular structure and the local ordering of the five-ring core in a series of banana mesogens, provided that reasonable estimates of CSA tensors of various carbon sites and the orientation of one wing with respect to the long molecular axis in the bent-core structure exist. In our case, the angle θ_{Cl} was estimated in a previous study by means of deuterium and ^{13}C NMR spectroscopy. When CSA tensors can be measured from the central phenyl ring, ^{13}C NMR can, in principle, give the angle θ_{Cl}. Preliminary results using the SUPER [29] (separation of undistorted CSA powder patterns by effortless recoupling) method have yielded $\delta_{11} = 27.4$, $\delta_{22} = 122.1$, and $\delta_{33} = 217.4$ (the 3-axis is taken along the C-Cl bond) for C_{10} in 10DClPBBC [30]. With this CSA, the predicted chemical shifts (dashed line) for this carbon site are shown in Fig. 6. This shows that this carbon site in the central phenyl ring can be used to give S directly and a direct measure of the θ_{Cl} angle (our 12° seems to be good) is possible in this mesogen. Because of the biphenyl fragments are nonplanar, it is possible that their twist senses are opposite in reference to the central phenyl ring, giving a propeller effect on the entire molecular core. Unfortunately, current ^{13}C NMR spectra are unable to confirm this conjesture, but it certainly opens up the question of achiral nature of banana mesogens.

[1] R. B. Meyer, L. Leibert, L. Strzelecki, and P. Keller, J. Phys. (France) Lett. **36**, L69 (1975).

[2] A. P. L. Chandani, Y. Ouchi, H. Takezoe, A. Fukuda, H. Tereshima, K. Furukawa, and A. Kishi, Jpn. J. Appl. Phys., Part 2 **28**, L1261 (1989).

[3] A. Fukuda, Y. Takanishi, T. Isozaki, K. Ishikawa, and H. Takezoe, J. Mater. Chem. **4**, 997 (1994).

[4] T. Niori, F. Sekine, J. Watanabe, T. Furukawa, and H. Takezoe, J. Mater. Chem. **6**, 1231 (1996).

[5] A. Jakli and P. Toledano, Phys. Rev. Lett. **89**, 275504 (2002).

[6] J. Xu, R. L. Selinger, J. V. Selinger, and R. Shashidhar, J. Chem. Phys. **115**, 4333 (2001).

[7] A. Eremin, I. Wirth S. Diele, G. Pelzl, H. Schmalfuss, H. Kresse, H. Nadasi, K. Fodor-Csorba, E. Gacs-Baitz, and W. Weissflog, Liq. Cryst. **29**, 775 (2002).

[8] G. Pelzl, S. Diele, and W. Weissflog, Adv. Mater. (Weinheim, Ger.) **11**, 707 (1999).

[9] E. Matyus and K. Fodor-Csorba, Liq. Cryst. **30**, 445 (2003).

[10] K. Fodor-Csorba, A. Vajda, G. Galli, A. Jakli, D. Demus, S. Holly, and E. Gacs-Baitz, Macromol. Chem. Phys. **203**, 1556

(2002).

[11] W. Weissflog, Ch. Lischka, S. Diele, G. Pelzl, I. Wirth, S. Grande, H. Kresse, H. Schmalfuss, H. Hartung, and A. Stettler, Mol. Cryst. Liq. Cryst. Sci. Technol., Sect. A **333**, 203 (1998).

[12] S. Diele, S. Grande, H. Kruth, Ch. Lischka, G. Pelzl, and W. Weissflog, Ferroelectrics **212**, 169 (1998).

[13] G. Pelzl, S. Grande, A. Jakli, Ch. Lischka, H. Kresse, H. Schmalfuss, I. Wirth, and W. Weissflog, Liq. Cryst. **26**, 401 (1999).

[14] H. Dehne, M. Potter, S. Sokolowski, W. Weissflog, S. Diele, G. Pelzl, I. Wirth, H. Kresse, H. Schmalfuss, and S. Grande, Liq. Cryst. **28**, 1269 (2001).

[15] H. Nadasi, W. Weissflog, A. Eremin, G. Pelzl, S. Diele, B. Das, and S. Grande, J. Mater. Chem. **12**, 1316 (2002).

[16] R. Y. Dong, K. Fodor-Csorba, J. Xu, V. Domenici, G. Prampolini, and C. A. Veracini, J. Phys. Chem. B (to be published).

[17] K. Fodor-Csorba, A. Vajda, A. Jakli, C. Slugovc, G. Trimmel, D. Demus, E. Gacs-Baitz, S. Holly, and G. Galli (unpublished).

[18] A. Bax and G. A. Morris, J. Magn. Reson. (1969-1992) **42**, 501 (1981).

[19] B. M. Fung, A. K. Khitrin, and K. Ermolaey, J. Magn. Reson. **142**, 97 (2000).

[20] X. Wu and K. W. Zilm, J. Magn. Reson., Ser. A **102**, 205 (1993).

[21] T. Nakai, H. Fujimori, D. Kuwahara, and S. Miyajima, J. Phys. Chem. B **103**, 417 (1999).

[22] A. Yoshizawa, H. Kikuzaki, and M. Fukumasa, Liq. Cryst. **18**, 351 (1995).

[23] D. E. Wemmer and A. Pines, J. Am. Chem. Soc. **103**, 34 (1981).

[24] G. Zheng, J. Hu, X. Zhang, L. Shen, C. Ye, and G. A. Webb, J. Mol. Struct.: THEOCHEM **428**, 283 (1998).

[25] D. E. Wemmer, A. Pines, and D. D. Whitehurst, Philos. Trans. R. Soc. London, Ser. A **300**, 15 (1981).

[26] W. H. Press, B. P. Flannery, S. A. Teukolsky, and W. T. Vetterling, *Numerical Recipes* (Cambridge University Press, Cambridge, England, 1986).

[27] I. V. Haller, Prog. Solid State Chem. **10**, 103 (1975).

[28] Y. Kinoshita, B. Park, H. Takezoe, T. Nion, and J. Watanabe, Langmuir **14**, 6256 (1998).

[29] S.-F. Liu, J.-D. Mao, and K. Schmidt-Rohr, J. Magn. Reson. **155**, 15 (2002).

[30] J. Xu and R. Y. Dong (unpublished).